Modelling the Combustion of Explosives

Sally Said [*], *John Curtis*[†], *Frank Smith*[‡]

[*]UCL Mathematics, s.said.17@ucl.ac.uk
[†]UCL Mathematics, AWE
[‡]UCL Mathematics

Abstract

When an explosive burns, gaseous products are formed as a result. The interaction of the burning solid and gas is not well understood. More specifically, the process of the gaseous product heating the explosive is yet to be explored in detail. The present work is aimed towards filling that gap using mathematical modelling: this aims to track the temperature profile in the explosive and the gas's response.

This work begins by modelling with finite difference methods the reaction-diffusion process assuming single step reactions using the simple Arrhenius model. An alternative asymptotic approach is also employed. There is close agreement between the results for the full reaction-diffusion problem and the asymptotic problem. The model is then extended to include three step reaction kinetics, where we again apply asymptotic analysis in addition to direct computation. Further work outlined briefly at the end includes the motion of gas being incorporated in the existing model with temperature and pressure distributions considered.

1 Introduction

High Explosives (HEs) store energy which can have disastrous effects if released accidentally. Thus safe handling and storage of HEs is a matter of utmost concern [1]-[2]. When a HE is subjected to significant heating it reacts, i.e. it burns to form gaseous products. The interaction of the burning solid and gaseous products formed is not well understood. More specifically, the process of the gaseous product heating explosives is yet to be explored in detail.The present work does much to fill that gap using mathematical modelling: this aims to track the temperature and volume profiles, as well as pressure distributions in the explosive and the gas response.

A detailed discussion on the technology of explosives can be found in [1] and [2], where the physical processes involved in explosives are explored in detail. This includes an insight into the chemical processes which occur as well as the mechanics of the burning process and detonation.

Modelling the combustion of explosives is a topic which has been studied for several decades [3], [4] and has received a lot of attention in recent years . It is widely accepted that the combustion process occurs in several stages which need to be studied. In particular the process of burning to detonation, or the deflagration-to-detonation transition (DDT) [5], is one which is not yet fully understood due to the complex chemistry involved. Understanding the DDT process is highly important for the development, as well as the safe handling and storage of explosives. The burning of primary explosives is often used as a detonation device for secondary explosives [1]. Most primary explosives readily detonate through thermal stimulus. Similarly secondary explosives can be used to detonate tertiary explosives. Unfortunately, however, understanding the time to detonation of the secondary explosive is much more complex. Often large time delays are encountered. There have been various theories on the mechanisms which drive the DDT process; [6] suggest the formation of shock waves ultimately result in detonation.

McGuire and Tarver [7] use a thermal conduction model to predict time to detonation compared with reciprocal temperature. It is well documented in the literature [8] that time to detonation cannot be predicted accurately with the single step Arrhenius reaction. The authors of [7] predict time to detonation for several confined explosives, namely; HMX, RDX, TATB and TNT. The reaction of explosives can be broken down into three processes, which are: an endothermic reaction, a slightly exothermic reaction and an extremely exothermic reaction. McGuire and Tarver [7] model these processes using a three step chemical decomposition model for the four explosives. The time to detonation compared is accurately predicted and verified against experimental results.

In the present article a brief description is provided of research currently in progress involving a collaboration between AWE and University College London. This is based on a doctoral project [17] by the first-named author and is supported by AWE and EPSRC UK through an Industrial CASE award. The article focusses on mathematical modelling, and its following sections address successively, within the context of a two-dimensional slab model, first the governing equations and then the solutions with a single reactant present, the solutions here being based on direct computation and /or the use of asymptotic analysis: comparisons between the two are included. Subsequently the work is extended to the more realistic or studied case of three reactants. Further work is also discussed.

2 The Governing Equations

In dimensional terms the governing equations of interest for the reaction-diffusion problem with a single reactant involved take the form

$$\rho c_v \frac{\partial u}{\partial t} = \kappa \frac{\partial^2 u}{\partial x^2} + \rho \Omega \frac{\partial \alpha}{\partial t}, \tag{1}$$

$$\frac{\partial \alpha}{\partial t} = A(1-\alpha) \exp\left(-\frac{E}{Ru}\right), \tag{2}$$

where ρ represents the density, c_v the specific heat, κ the conductivity, Ω the heat of the reaction, A the pre-exponential constant, E the activation energy required for the reaction to begin, while u is the temperature and α is the reaction rate. Some of these parameters take extremely large or small values in practice and for that reason we will turn to a non-dimensional form of the governing equations shortly. Meanwhile a sample of three solutions of the system (1)-(2) obtained numerically from a finite-difference treatment that preserves second-order accuracy is presented in Figure 1. To describe the treatment in brief, we observe that a semi-implicit method for the present nonlinear evolution problem is appropriate here for the sake of numerical stability coupled with accuracy; a three-point backward differencing scheme is applied to facilitate the second order accuracy in time whereas a centred difference procedure is used for the second-order accuracy spatially. For instance the contribution from the time derivative in (1) is discretised according to

$$\frac{\partial u}{\partial t} \approx \frac{3U_{j,i} - 4U_{j,i-1} + U_{j,i-2}}{2\Delta t} \tag{3}$$

in a schematic sense, and similarly for the other terms in the governing equations. The results indicate boundary-layer-like effects are taking place, i.e. the numerical solution varies considerably (abruptly) in thin layers very close to the edges of the computational domain. Outside those layers the development of the numerical solutions for u, α is much more gradual and smooth, with the temperature eventually increasing to comparatively high values as time progresses further.

In order to deal with the effects of the many parameters involved we introduce the non-dimensional/scaled variables $\bar{t}$ and $\bar{u}$ that satisfy

$$t = A^{-1}\bar{t}, \qquad u = \frac{E}{R}\bar{u}, \tag{4}$$

having recognised the fact that A is likely to be responsible for change in u and α happening on different time scales, and that $\frac{E}{R}$ is relatively large. Note that we do not need to scale α since it is already non-dimensional and $\mathcal{O}(1)$.

Substituting the scalings (4) into the PDEs above yields the new scaled system of non-dimensional PDEs

$$\frac{\partial \bar{u}}{\partial \bar{t}} = \bar{\kappa} \frac{\partial^2 \bar{u}}{\partial x^2} + \bar{\Omega} \frac{\partial \alpha}{\partial \bar{t}}, \tag{5}$$

$$\frac{\partial \alpha}{\partial \bar{t}} = (1-\alpha) \exp\left(-\frac{1}{\bar{u}}\right), \tag{6}$$

where $\bar{\kappa} := \frac{\kappa}{\rho c_v A}$, and $\bar{\Omega} := \frac{\Omega R}{c_v E}$. The boundary and initial conditions now become

$$\begin{aligned} \bar{u}(-1,t) = \bar{u}(1,t) = \bar{B}, &\quad \text{for } 0 < \bar{t} \le T_{\max}, \\ \bar{u}(x,0) = \bar{D}, &\quad \text{for } -1 < x < 1, \end{aligned} \tag{7}$$

where $\bar{B} := \frac{RB}{E}$ and $\bar{D} := \frac{RD}{E}$. Here B is the Dirichlet boundary condition, $B = 570$ at $x = \pm 1$, D is the initial condition $D = 293$ and T_{max} is the period of time over which we model the event. Note that the initial condition for α remains unchanged.

A sample solution of (5)-(6) derived numerically using the same approach as previously is presented in Figure 2. Also however by scaling or non-dimensionalising the variables u and t, we have successfully

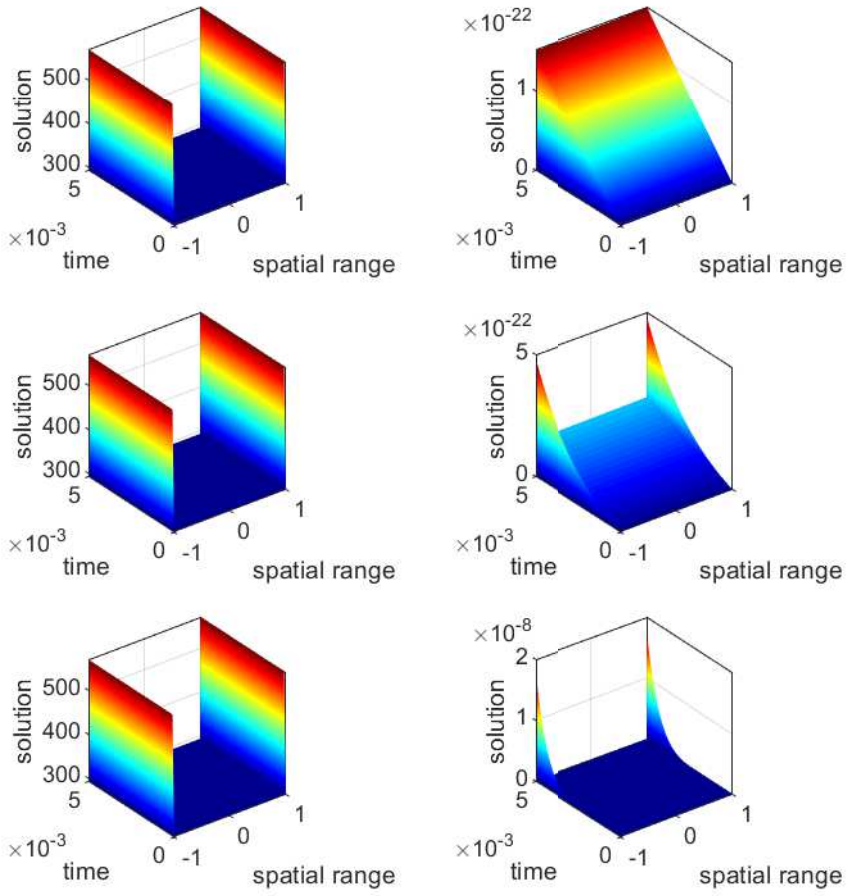

Fig. 1: The numerical finite difference solutions to u (left) and α (right) from the PDEs (1)-(2). We chose the discretisation parameters $\Delta t = 0.0001$, $N_x = 1000, 10000, 100000$ (top–to–bottom) and $T_{max} = 0.05$. Note how α is extremely sensitive to our choice of N_x.

scaled out most of the extreme parameters and reduced the PDEs (1)-(2) to (5)-(6) with coefficients that are approximately $\mathcal{O}(1)$ (excluding $\bar{\kappa}$). The corresponding boundary conditions are also $\mathcal{O}(1)$ along with the unscaled variable α. To address the effects of the very small parameter $\bar{\kappa}$ that still features in the scaled PDE and is non-dimensional we may now also take a different approach. It can be shown through asymptotic expansions of $\bar{u}$ and α [9] that by equating the coefficients of like powers of $\bar{\kappa}$ and taking $\mathcal{O}(1)$ terms only, the term $\frac{\partial^2 \bar{u}}{\partial x^2}$ is unlikely to have any substantial effect for a long time, except near the boundaries, since the reaction term dominates. Hence, asymptotically, the problem can now be viewed as the interaction of two problems; a problem in thin wall layers at both ends of the domain and a problem in a core.

3 Comparison between direct computation and asymptotic analysis

Concerning the analysis, in the core, the term $\frac{\partial^2 \bar{u}}{\partial x^2}$ in (5) has virtually no effect and therefore we may instead study the reduced PDE

$$\frac{\partial \overline{u}}{\partial \overline{t}} = \overline{\Omega} \frac{\partial \alpha}{\partial \overline{t}}, \tag{8}$$

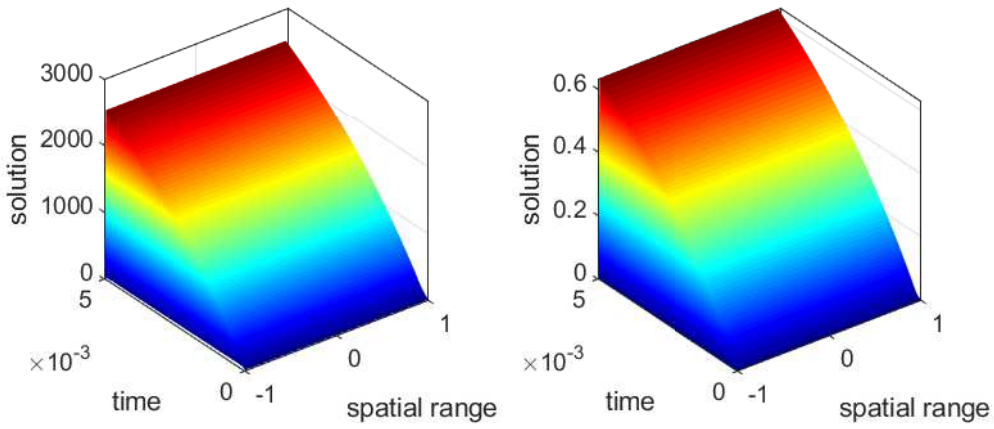

Fig. 2: The numerical finite difference solutions to $\bar{u}$ (left) and α (right) from the PDEs (5)-(6) with mild physical parameters.

which, to our favour, admits a simple analytical solution. We have that

$$\bar{u} = \bar{\Omega}\alpha + c_1, \tag{9}$$

in the core, where c_1 is a constant of integration to be determined. By the term 'core' we mean that $-1+\epsilon < x < 1-\epsilon$ for some $\epsilon \ll 1$. In other words, the core solution is valid on practically all of the domain, except for thin layers of width $\mathcal{O}(\epsilon)$ near the boundaries, where $\frac{\partial^2 \bar{u}}{\partial x^2}$ does influence the solution (see below). In terms of matched asymptotic expansions we comment that we would expand $\bar{u} = \bar{u}_0 + ...$, $\alpha = \bar{\alpha}_0 + ...$ and equate terms of equal orders in the original governing equations to obtain equations for the subscript-zero quantities but the latter equations at leading order turn out to be the same as the two equations displayed above, Equations (8) and (9).

Applying the initial conditions $\bar{u}(x,0) = \bar{D}$ and $\alpha(x,0) = 0$ yields

$$\bar{u}(x,\bar{t}) = \bar{\Omega}\alpha(x,\bar{t}) + \bar{D}, \tag{10}$$

for $-1+\epsilon < x < 1-\epsilon$ and $\bar{t}$ of order unity, and thus the equation (6) becomes (in the core)

$$\frac{\partial \alpha}{\partial \bar{t}} = (1-\alpha)\exp\left(-\frac{1}{\bar{\Omega}\alpha + \bar{D}}\right). \tag{11}$$

Note that since the initial condition $\alpha(x,0) = 0$ is independent of x, (11) as it stands is also independent of x and essentially represents a non–linear ODE for α that is valid for $-1+\epsilon < x < 1-\epsilon$, including at the edge of the thin wall layer as x closely approaches -1 and 1. (We remark in passing here that x-dependence in the initial conditions at $t = 0$ would be reflected in $\bar{D}$ in (10), (11) and similarly $\alpha(x,0)$ being given functions of x; this could be of future interest.) As a result, the core solutions provide 'inside' boundary conditions for corresponding $\bar{u}$ and α that satisfy the accompanying wall problems (to be discussed in the following section). The ODE (11) is nontrivial to solve and so we use `ODE45` in MATLAB to integrate numerically. The core reaction α may then be substituted back into (10) to determine the leading order u in the core.

In Figure 3 we plot the core solutions $\bar{u}$ and α that satisfy (10) and (11), respectively, using the mild parameter values $E = 10$ and $A = 200$ as well as $D = 15$ which is required for the initial condition of $\bar{u}$. The asymptotic analysis is still valid using these mild parameters since the corresponding value of $\bar{\kappa}$ is still exceptionally small. We use mild parameters for now so that in a sense we may validate (see Figure 6) the asymptotic analysis against the finite difference solutions given in Figure 2, before proceeding to employ the

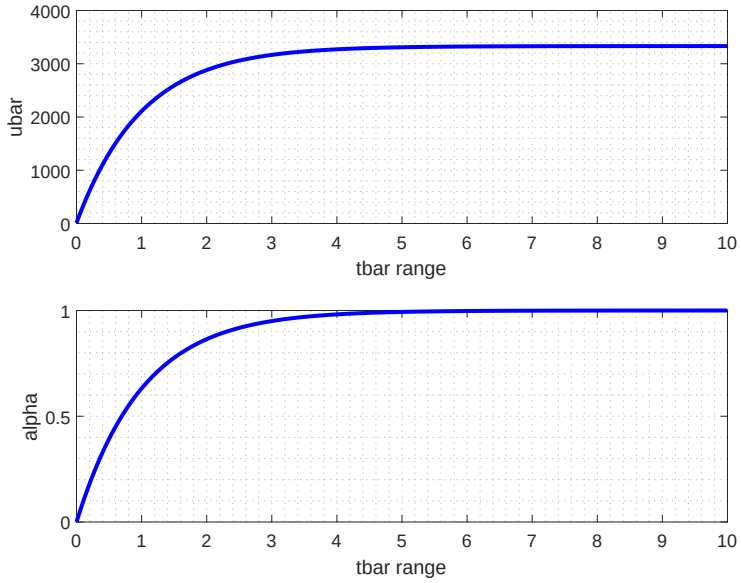

Fig. 3: The numerical approximations (using `ODE45` in MATLAB) to $\bar{u}$ and α in the core satisfying (10) and (11) with the mild parameter values $E = 10$, $A = 200$ and $D = 15$ and hence $\bar{D} = 12.471$, $\bar{\Omega} = 3319.5$.

full parameter values.

The core equations have no spatial dependence and are in fact only initial value problems. As a result, the loss of the derivative term in x means that the underlying boundary conditions in (7) cannot be satisfied in the core, in the general case. Hence we seek an accompanying solution to the core solutions by considering the system (5)-(6) near the boundaries. As alluded to previously, we term this second problem the wall or wall layer problem.

To handle the extreme parameter $\bar{\kappa}$ we set, near the left hand boundary,

$$x = -1 + \bar{\kappa}^{\frac{1}{2}}\bar{x}$$

and transform the problem (5)-(6) on $-1 \leq x \leq 1$ to a problem on $0 \leq \bar{x} < \infty$ that essentially provides a solution in the thin wall layer there. A representative value of $\bar{\kappa}$ is of the order $\mathcal{O}(10^{-20})$ and in a sense this tends to reflect the relatively poor conductivity of the slab material in many cases. From substitution, the system (5)-(6) becomes

$$\frac{\partial \bar{u}}{\partial \bar{t}} = \frac{\partial^2 \bar{u}}{\partial \bar{x}^2} + \bar{\Omega}\frac{\partial \alpha}{\partial \bar{t}}, \qquad \frac{\partial \alpha}{\partial \bar{t}} = (1-\alpha)\exp\left(-\frac{1}{\bar{u}}\right), \tag{12}$$

in the wall layers, where $\bar{\Omega} = \frac{\Omega R}{c_v E}$ again. Essentially the same system also applies at the edge layer near $x = 1$ after scaling.

It is notable that since the core problem is independent of x, the solutions at the inside edges of the wall layers (that is, at large $\bar{x}$) are valid across the entire core. In other words, the solutions $\bar{u}$ and α satisfying (12) coincide with the core solutions at $\bar{x} = \infty$. We therefore subject (12) to the boundary conditions

$$\bar{u}(\infty, \bar{t}) = \bar{u} \text{ in the core}, \qquad \alpha(\infty, \bar{t}) = \alpha \text{ in the core},$$

for $0 < \bar{t} \leq \bar{T}_{\max}$ or $\bar{t}$ of $\mathcal{O}(1)$. Here $\bar{T}_{\max}(\gg 1)$ is the period of time over which we model the event. It also

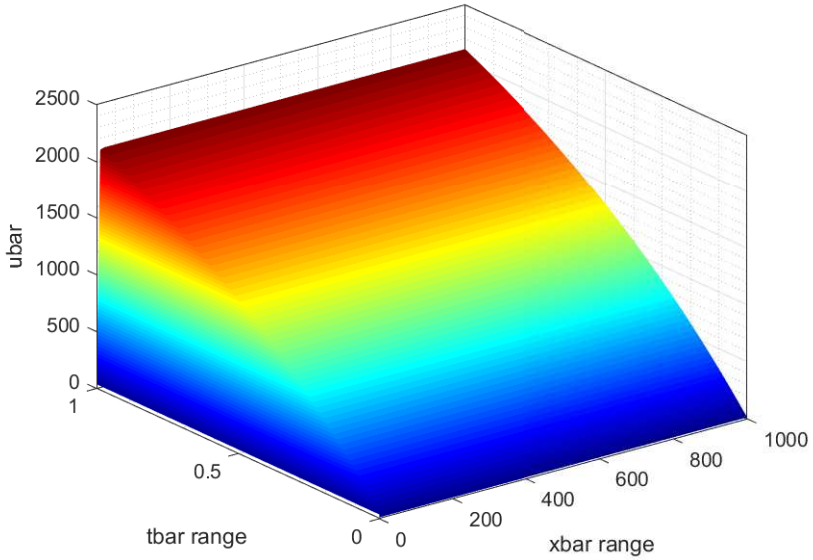

Fig. 4: The wall solution $\bar{u}$ satisfying (12) with the mild parameters $E = 20$; $A = 200$; $D = 15$ and $B = 45$. Note that the $\bar{x}$ range has been truncated to facilitate a numerical implementation.

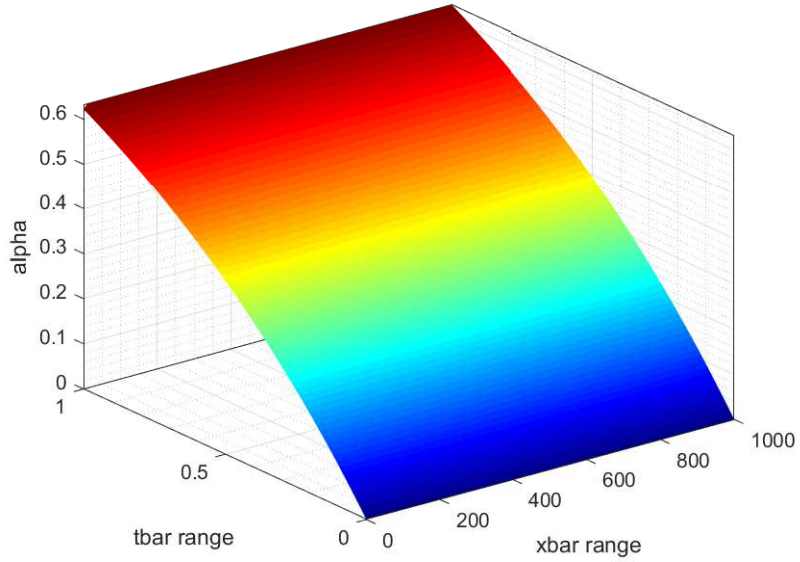

Fig. 5: The wall solution α satisfying (12) with the mild parameters $E = 20$; $A = 200$; $D = 15$ and $B = 45$. Note that the $\bar{x}$ range has been truncated to facilitate a numerical implementation.

holds that

$$\bar{u}(0, \bar{t}) = \bar{B}, \qquad \bar{B} = \frac{RB}{E}, \tag{13}$$

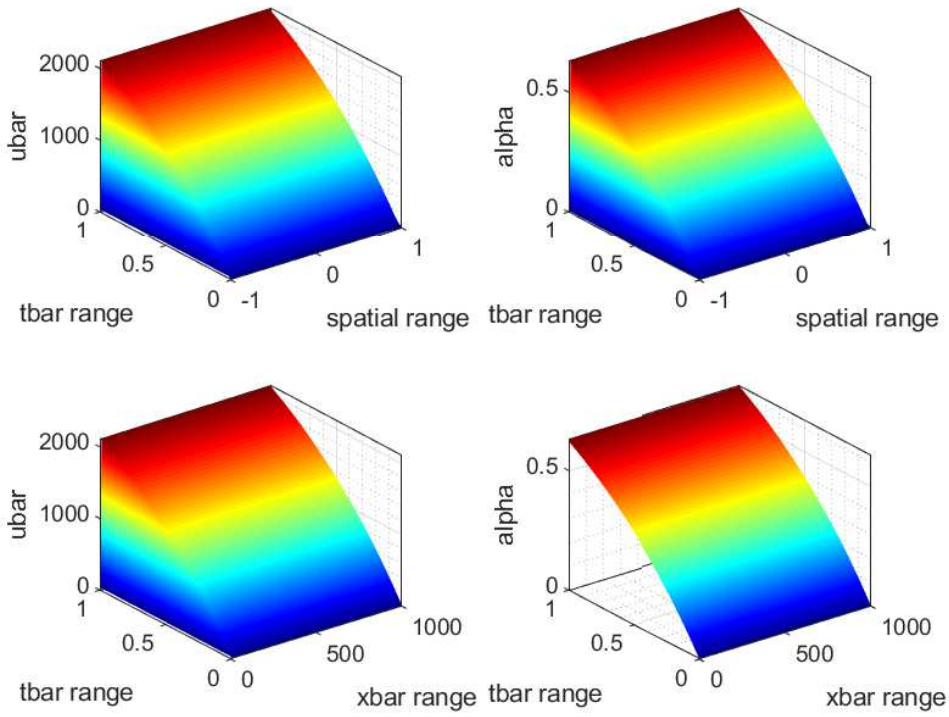

Fig. 6: Finite difference solutions to the full non–asymptotic problem shown in Figure 2 (top) and the asymptotic wall problem (bottom) using the mild parameters $E = 20$; $A = 200$; $D = 15$ and $B = 45$. For the non–asymptotic problem we set $T_{\max} = 0.005$. In order to compare the solutions directly we multiply the non asymptotic u by $\frac{R}{E}$ and $T_{\max}$ by A (resulting in $0.005 \times 200 = 1$, i.e. the time durations now match).

and the boundary conditions for α at the wall $\bar{x} = 0$ can be determined by solving the second equation in (12) using the condition (13). That is, we simply solve

$$\frac{\partial \alpha}{\partial \bar{t}} = (1 - \alpha) \exp\left(-\frac{E}{RB}\right),$$

which yields, at the wall,

$$\alpha(\bar{x}, \bar{t}) = 1 - \exp\left(-\bar{t} \exp\left(-\frac{E}{RB}\right)\right), \tag{14}$$

for $\bar{x} = 0$ and $0 < \bar{t} \leq T_{\max}$. We also have the initial conditions

$$\bar{u}(\bar{x}, 0) = \bar{D}, \qquad \alpha(\bar{x}, 0) = 0, \qquad 0 < \bar{x} < \infty.$$

We observe that there is a similarity solution for small times $\bar{t}$ near $\bar{x} = 0$. To solve numerically the system (12) we use the finite difference scheme of the previous section. In Figures 4 and 5 we plot the finite difference approximations to $\bar{u}$ and α using the mild parameters $E = 20$; $A = 200$; $D = 15$ and $B = 45$. In Figure 6 we compare the full non–asymptotic solutions given in Figure 2 (top) with the new asymptotic wall solutions (bottom). The spatial uniformity observed in many of the figures is largely due to the initial conditions, as explained by the accompanying study of asymptotic properties holding for small values of $\bar{\kappa}$.

We finish here by remarking that the present asymptotic methodology could serve as a reasonable alternative to the use of full numerical simulations in the diffusion-reaction systems of interest.

4 Multi-kinetics

The single reactant case serves as a reasonable first model for generating ideas for example but on the other hand it is well established in the literature that single reactants have many limitations when modelling the combustion of explosives. One such limitation is the over simplification of the chemical processes which take place during combustion. In this section we introduce a multi kinetic reaction process into our model. This provides a better representation of the physical and chemical processes which occur, see [1] for detail. Following the work of [7], [10] and [11] for example, we consider a three step reaction to model the endothermic and exothermic chemical processes. Consider the model equation

$$\rho c_v \frac{\partial u}{\partial t} = \kappa \frac{\partial^2 u}{\partial x^2} + \\ + N_A Q_1 Z_1 \exp\Big(-\frac{E_1}{Ru}\Big) + N_B Q_2 Z_2 \exp\Big(-\frac{E_2}{Ru}\Big) + N_C^2 Q_3 Z_3 \exp\Big(-\frac{E_3}{Ru}\Big) \tag{15}$$

which describes the diffusion process with a three-step reaction. We have the following ODEs, describing the rate of change of the reactions N_A, N_B and N_C respectively

$$\dot{N_A} = -\frac{N_A Z_1}{\rho} \exp\Big(-\frac{E_1}{Ru}\Big), \tag{16}$$

$$\dot{N_B} = \frac{N_A Z_1}{\rho} \exp\Big(-\frac{E_1}{Ru}\Big) - \frac{N_B Z_2}{\rho} \exp\Big(-\frac{E_2}{Ru}\Big), \tag{17}$$

$$\dot{N_C} = \frac{N_B Z_2}{\rho} \exp\Big(-\frac{E_2}{Ru}\Big) - \frac{N_C^2 Z_3}{\rho} \exp\Big(-\frac{E_3}{Ru}\Big), \tag{18}$$

where dots denote derivatives with respect to time.

Computational solutions for the three-reactant case are given in Figure 7. Asymptotic analysis not discussed in detail here but founded on the techniques described previously in section 3 provides further understanding again.

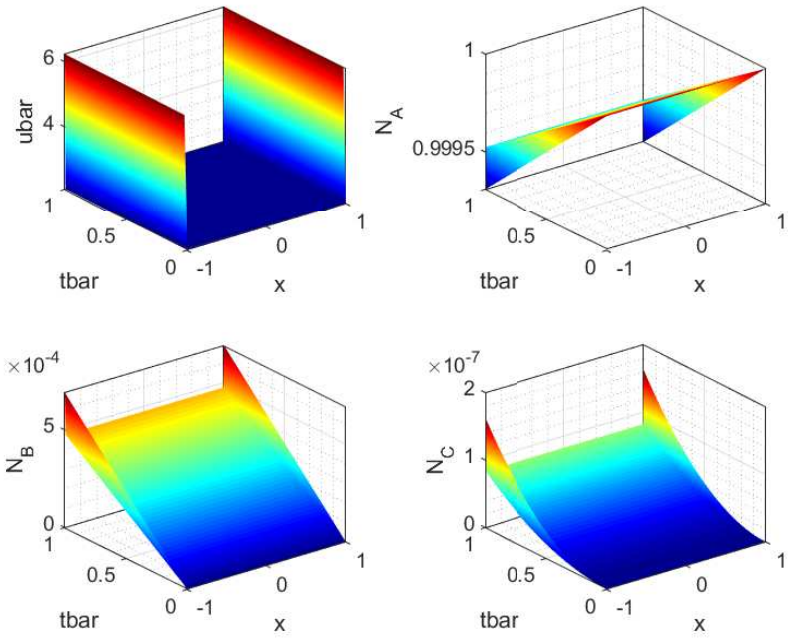

Fig. 7: Finite difference solutions to the full non–asymptotic problem shown using mild parameters.

5 Final comments

Keeping the final comments brief at this stage, we remark first that the combined use of direct computation and analysis for the model problems in this article appears to be promising as far as understanding of the physical processes is concerned. It remains to be seen whether the above combination works well in regard to reasonable prediction of events that occur in practice. Second, there is still much intriguing work to be done to fulfill that promise for the present model tasks. Third, future studies in particular on an extension of the present approach to allow for fluid-dynamical influences in the interactions are planned.

5.1 Acknowledgements

Thanks are due to AWE and EPSRC for financial support of SS during this research (EPSRC grant reference EP/R512138/1) and to several colleagues at UCL and AWE for interesting discussions.

References

[1] P. W. Cooper and S. R. Kurowski, *Introduction to the Technology of Explosives*. 1996.

[2] P. W. Cooper, *Explosives engineering*. 1996.

[3] F. Williams, *Combustion Theory*. Addison-Wesley series in engineering sciences, Addison-Wesley Publishing Company, 1965.

[4] M. Ward, S. Son, and M. Brewster, "Steady Deflagration of HMX With Simple Kinetics: A Gas Phase Chain Reaction Model," 1997.

[5] P. E. Luebcke, P. M. Dickson, and J. E. Field, "Deflagration-to-Detonation Transistion in Granular Pentaerythritol Tetranitrate," *J. Appl. Phys.*, vol. 79, no. 7, pp. 3499–3503, 1996.

[6] J. M. Groocock, "Griffiths and Groocock : The Burning to Detonation of Solid Explosives," no. 4154, 1958.

[7] R. R. McGuire and C. M. Tarver, "Chemical Decomposition Models for the Thermal Explosion of Confined HMX, TATB, RDX, and TNT Explosives," *Symposium on Detonation*, no. June, p. 11, 1981.

[8] C. Tarver, R. McGuire, E. Lee, E. Wrenn, and K. Brein, "The thermal decomposition of explosives with full containment in one-dimensional geometries," *Symposium (International) on Combustion*, vol. 17, no. 1, pp. 1407 – 1413, 1979. Seventeenth Symposium (International) on Combustion.

[9] S. Bullett, T. Fearn, and F. Smith, *Advanced Techniques in Applied Mathematics*. WORLD SCIENTIFIC (EUROPE), 2016.

[10] J. Curtis, "A new analytical model of the one-dimensional time to explosion experiment," *Unpublished AWE Report*, October 2018.

[11] S. Said, "Modelling the combustion of explosives," *PhD thesis in progress, University College London*.